

## Flamingo technique as an innovative method to improve the shear capacity of reinforced concrete beam

Suhad M. Abd<sup>a</sup>, Isam S. Mhaimeed<sup>a,\*</sup>, Bassam A. Tayeh<sup>b</sup>, Hadee Mohammed Najm<sup>a</sup>, Shaker Qaidi<sup>c,d</sup>

<sup>a</sup> University of Diyala, College of Engineering, Baqubah, Diyala, Iraq

<sup>b</sup> Civil Engineering Department, Faculty of Engineering, Islamic University of Gaza, Gaza Strip, Palestine

<sup>c</sup> Department of Civil Engineering, College of Engineering, University of Duhok, 42001 Duhok, Iraq

<sup>d</sup> Department of Civil Engineering, College of Engineering, Nawroz University, 42001 Duhok, Iraq



### ARTICLE INFO

**Keywords:**

Shear failure  
Flamingo technique  
Inclination  
Free ends  
Ductility  
Shear capacity

### ABSTRACT

The sudden incidence of shear failure in the structural elements of the concrete entails using shear reinforcement in order to enhance the ductility. This study presents the use of an innovative steel reinforcement technique in reinforced concrete beams. The steel bars were composed in a form like that of the flamingo bird. Five beams with dimensions of 200 mm x 300 mm x 1500 mm were cast, cured, and evaluated in shear under four-point bending. One beam has been reinforced using the conventional steel stirrups as a control beam, while the new flamingo technique reinforced the other four beams in the shear zone with the parameters of variation in the inclination and lengths of the lower and upper free ends. The results revealed that the use of the flamingo technique has perfectly increased the shear capacity of the beam, and ultimate deflection, increased the shear ductility and decreased the crack width.

### 1. Introduction

Concrete shear reinforcement improves ductility and prevents sudden shear failure. Diagonal cracks start near the supports and extend to the top zone, indicating shear failure. Consequently, the intersection caused by any reinforcement type restricts diagonal crack extension and resists shear forces to a certain limit. Steel reinforcement bars are shear reinforcements (i.e., stirrups). Steel stirrups are used to resist high shear stresses in beams [1–3].

Many studies exhibit the efficiency of using different shear reinforcement techniques such as steel plate [4–7], steel strip [8,9], swimmer bar [5,10–12], and lacing reinforcement instead of the traditional steel stirrups [13]. However, steel plate and steel strip techniques have differed from the other techniques since they adopted new forms of steel material in reinforcing the structural members in shear despite their use with an equivalent area to the traditional steel stirrups. The swimmer bar and lacing reinforcement techniques represent conventional steel bars in irregular forms. In contrast, the swimmer bar system is a new shear reinforcement technique in which the small-sized bars are inclined with the two ends bent horizontally while both are welded to the lower and upper longitudinal steel reinforcement.

The swimmer bars were also used to reinforce the flat plates in order to resist punching shear failure [14]. The results have shown that using swimmer bars improves the punching shear strength by 8.3% and increases the slab's rigidity. Furthermore, the slab

\* Corresponding author.

E-mail address: [isam\\_saleem\\_eng\\_civil@uodiyala.edu.iq](mailto:isam_saleem_eng_civil@uodiyala.edu.iq) (I.S. Mhaimeed).

thickness can be reduced with the use of spaced swimmer bars. Also, the drop panel can be avoided.

Lacing can be described as a continuous form of shear reinforcement that differs from the traditional steel stirrups in that it has been placed in the major bending plane and anchored by the cross bars [15]. The lacing reinforcement was used by Srinivasa Rao, Sarma, Lakshmanan and Stangenberg [15] in reinforcing 20 cantilever beams subjected to cyclic and monotonic loads. Several forms of lacing reinforcement, such as inclined-welded lacing, inclined bolted lacing, single-leg lacing, and rectangular lacing, were used as shear reinforcement. They concluded that the inclined lacing form provided a better response, and that the lacing reinforcing system can be effectively used to secure ductile failure even in the presence of high cyclic shear. Using a lacing bar system as shear reinforcement in reinforced concrete elements results in large deflections and promotes reinforcement by its strain hardening stage [16–18]. Madheswaran, Gnana Sundar and Gopalakrishnan [19] studied the ductile behaviour of the laced reinforced geopolymers concrete beam (LRGPC) with the ratio of shear span-to-depth  $< 2.50$  since ductile failure cannot be achieved with the use of the traditional steel stirrups below this ratio [11,20,21]. Subsequently, they enhanced the ductile failure of the beams by using the inclined lacing bars. Allawi and Arshad [22] investigated the lacing reinforcement effect on the flexural behaviour of 1-way slabs.

Generally, this study presents the use of the new technique of shear reinforcement, “which is the flamingo technique, since it is formed like the flamingo bird, while Kueres, Ricker and Hegger [23] investigated this reinforcement system for the first time. He developed a new punching shear reinforcement, which has been used for footings due to the steeper inclination of the shear cracks, which required punching shear reinforcement with inclined bars rather than vertical bars. The shear crack widths can be efficiently controlled with the new element of the punching shear reinforcement (Fig. 1a) in the reason for the inclination of various sections. Hence, shear cracks are crossed several times (Fig. 1b). Moreover, the punching shear reinforcement’s perfect activation is achieved by the reinforcement element’s rigid anchoring. Kueres, Ricker and Hegger [23] performed 15 tests on the footings of the reinforced concrete using a new punching shear reinforcement element according to different influencing parameters, including concrete compressive strength, shear span-depth ratio ( $a/d$ ), column perimeter-depth ratio ( $u/d$ ), longitudinal reinforcement at compression side, and diameter and layout of the punching shear reinforcement. Results showed that the use of the new punching shear reinforcement increases the punching shear strength for the foot by about 35% compared with the traditional stirrups” [24]. Fig. 2(a, b, and c) shows three modes of punching shear failure.

The recent study investigates the use of the flamingo shear reinforcement in reinforcing the concrete beam with different lengths at both lower and upper ends and various inclinations; the next section exhibits the experimental work, results, and discussion.

## 2. Method

### 2.1. Concrete mix

The ACI method for concrete mix design was used for a mix with a 28-day compressive strength ( $f_c$ ) of 40 MPa and a slump value of 130 mm. Table 1 shows the concrete mix constituents used in this work.

### 2.2. Flexural and shear reinforcement

Table 2 shows the “deformed steel bars of different sizes used in reinforcing the beams in shear and bending. Consequently, the  $\varnothing 8$  mm is used as stirrups in the control beam. In contrast,  $\varnothing 6$  was used in the fabrication of the flamingo technique with an equivalent

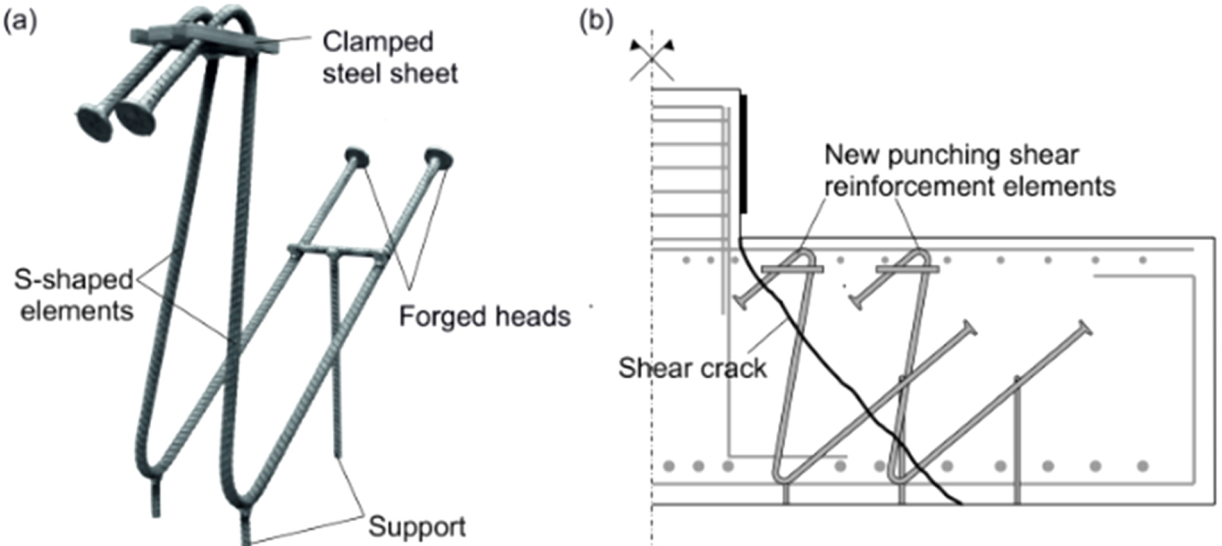


Fig. 1. New punching shear reinforcement element.

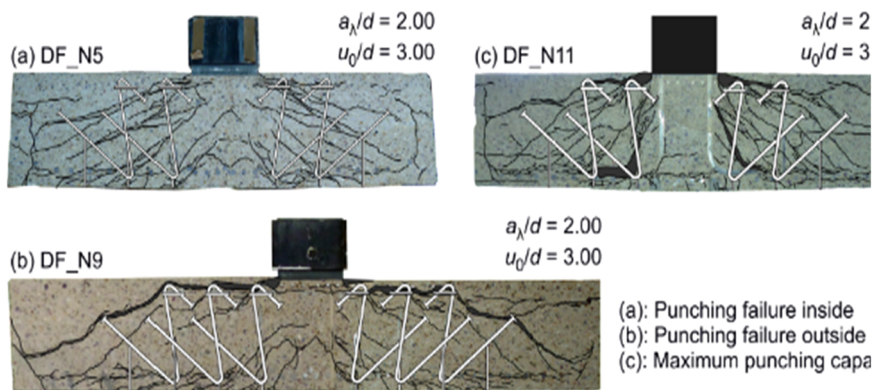


Fig. 2. Punching failure modes.

**Table 1**  
Concrete mix constituents.

Designation C40						
“Cement (kg/m <sup>3</sup> )	Sand (kg/m <sup>3</sup> )	Gravel (kg/m <sup>3</sup> )	Water (kg/m <sup>3</sup> )	S.P	w/c	Slump (mm)
450	860	860	252	0.33%	43%	130 mm”

area as compared with that of  $\varnothing 8$  mm,  $\varnothing 16$  as flexural reinforcement, and  $2 \varnothing 12$  are placed at the compression zone to stabilise the steel and carbon yarn stirrups (it is a fibre collected to form a bundle, then twisted and drew around the longitudinal main reinforcement like the traditional steel stirrups). The concrete cover for all is 25 mm. Fig. 3 shows the reinforcement details for the control beam. Fig. 4(a, b, and c) shows the schematic diagram for the beams reinforced with the flamingo technique and details of the reinforced section with the 3D model” [24].

### 2.2.1. Fabrication of Flamingo model

The following procedures show the fabrication of the flamingo reinforcement model: (i) The first step is represented by the preparation of the Z-shapes with the various angles of inclination ( $30^\circ$ ,  $40^\circ$ , and  $60^\circ$ ) for the lower and upper free ends in the horizontal direction (see Fig. 5). However, both of these ends differed in length, (ii) Weld the head stud to the free ends (doubly head), as shown in Fig. 6, and (iii) Finally, “the models are welded to the upper and lower longitudinal reinforcement, as shown in Fig. 7”.

## 3. Experimental programme

Ordinary wood of 25 mm thickness and moulds with dimensions of  $200 \text{ mm} \times 300 \text{ mm} \times 1500 \text{ mm}$  were used to “cast the beam specimens. The mould’s internal walls and base have been oiled to inhibit the concrete’s adhesion with them. One control beam in which the traditional steel stirrups are used, while the other four beams are reinforced by the flamingo technique and symbolised by  $F_x \% y \% \Theta$ , where  $x\%$  and  $y\%$  represent the ratio of the length of the lower and upper free ends to the distance limited by the centre of the top and bottom longitudinal reinforcement” [24]. Table 3 lists the beam specimen details.

## 4. Instrumentation

The central deflection was measured at any applied load by using the LVDT. Strain gauges were installed on the steel reinforcement to monitor the strains with applied force. Table 4 illustrates the characteristics of both strain gauge types. The strain gauge location was installed at the centre of the main reinforcement (flexural reinforcement) from the bottom and in the middle of each shear reinforcement stirrup, while for flamingo reinforcement, it was installed in the middle of each free end. For measuring the width of the

**Table 2**  
Properties of reinforcing steel bars.

“Nominal diameter (mm)	Cross-section Area (mm <sup>2</sup> )	$f_y$ (MPa)	$f_u$ (MPa)
8	50.24	450	747
12	113.04	425	700
6	28.26	400	720”

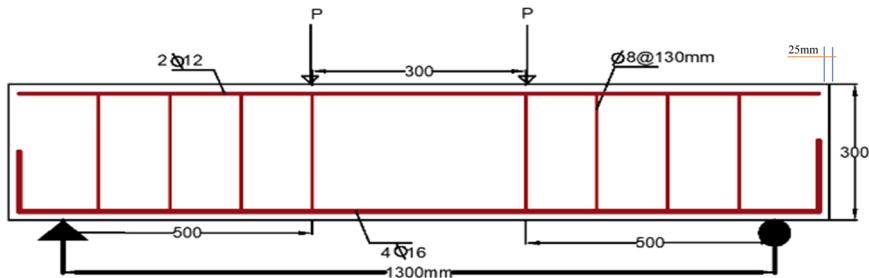
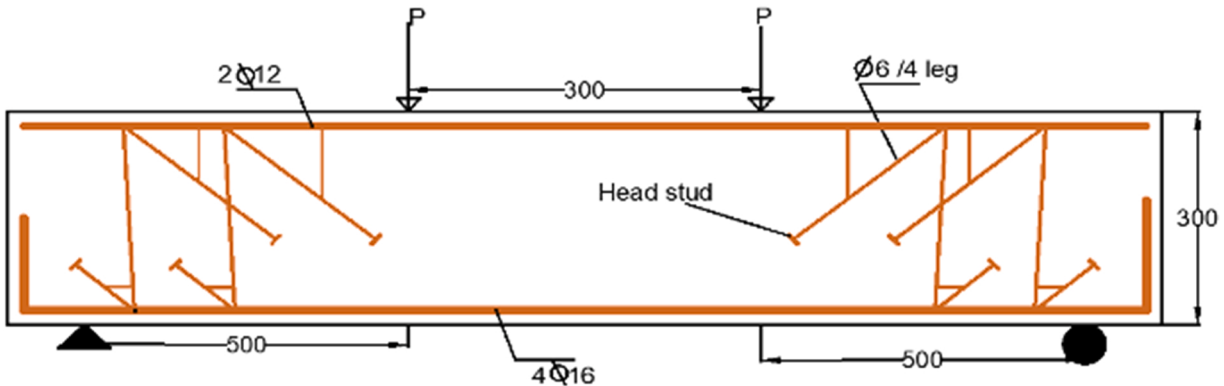
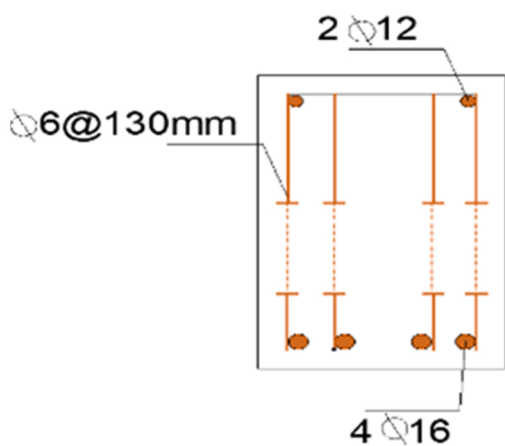


Fig. 3. Reinforcement details for the control.



a: Schematic diagram for beams which the flamingo technique has reinforced.



b: Cross-section



c: 3 D model

Fig. 4. Reinforcement details for the beam.

crack, an optical micrometre with a 0.02 mm accuracy has been utilised for all of the beam specimens. The surfaces of the beam have been painted white to make it easier to see the crack and measure the width.

## 5. Results and discussion

### 5.1. Load-carrying capacity

Table 5 shows the test results for all beams. “It can be observed that the use of the flamingo reinforcement system leads to an increase in the load-carrying capacity for the F<sub>1</sub> 60% 80% 30°, F<sub>2</sub> 60% 80% 40°, F<sub>3</sub> 60% 80% 60°, and F<sub>4</sub> 45% 75% 40° by 47%, 42.72%, 30.3%, and 24.85% respectively, as compared with the RCWS. However, the four flamingo beams were reinforced in shear, with the reinforcement area equal to that of the reference beam. This is attributed firstly to the frequent intersections that the flamingo



Fig. 5. Cutting process and forming.



Fig. 6. Welding heads on the free ends.



Fig. 7. Details of all specimens.

**Table 3**  
Details of tested beams [24].

Specimen	Description	Specimen Type
RCWS	Using $\varnothing 8$ steel stirrups mm at 130 mm	Control beam
F1 60% 80% 30°	With 60% lower-end length and 80% upper-end length with a 30° angle of inclination	
F2 60% 80% 40°	With 60% lower-end length and 80% upper-end length with a 40° angle of inclination	
F3 60% 80% 60°	With 60% lower-end length and 80% upper-end length with a 60° angle of inclination	
F4 45% 75% 40°	With 45% lower-end length and 75% upper-end length with a 40° angle of inclination"	

**Table 4**

Properties of strain gauges.

Type of the Gauge	Resistance in $\Omega$	Size of the Grid (mm)	Dimensions of the Gauge	
			Length (mm)	Width (mm)
BF350-1AA	120	1 × 3.75	4.7	4.6
BF120-20AA	120	20 × 3.50	25	5"

system legs achieved across the shear crack path, which restricts the crack propagation, and secondly to the inclination of both the lower and upper free ends. Nonetheless, the ultimate load of the F<sub>2</sub> 60% 80% 40° and F<sub>3</sub> 60% 80% 60° decreased gradually with the increase in the angle of the inclination of lower and upper free ends for the reason of the space that the upper free end realised with the increase in the inclination. Hence the concrete has only resisted the stresses in this zone. The beam F<sub>4</sub> 45% 75% 40° showed a high reduction in shear strength despite that it is with the same inclination of F<sub>2</sub> 60% 80% 40°. The sudden drop in the shear strength is attributed to the 15% decrease in the length of the lower free end. The table also illustrates the ultimate deflection values for the last five beams. The beam F<sub>1</sub> 60% 80% 30° showed a 40.15% increase in deflection compared to the control beam RCWS. This is attributed to the longitudinal reinforcement's plastic deformation since the beam failed in flexure. While the beam F<sub>2</sub> 60% 80% 40° showed a minor deflection increase compared with the control beam RCWS. This belongs to the increase in the post-cracking stiffness that the last yields. On the other hand, both F<sub>3</sub> 60% 80% 60° and F<sub>4</sub> 45% 75% 40° presented a reduction in the ultimate deflection valued by 18% – 19% in spite of their as compared with the control beam RCWS. This is attributed to the excellent post-cracking stiffness that the two beams present" [24].

### 5.2. Load-deflection behaviour

Fig. 8 illustrates the load-deflection behaviour for five beams; as can be seen, all curves are identical in the region bounded by the load inception until the load of 20 kN. The response is characterised by linearity during this stage since the concrete is still uncracked. However, the curve of the beam F<sub>4</sub> 45% 75% 40° is separated beyond this load to yield lower deflection in comparison with the other curves at the same load for the reason of the higher stiffness that the former showed. While the post-cracking stiffness is decreased gradually for the F<sub>1</sub> 60% 80% 30°, F<sub>2</sub> 60% 80%, 40° F<sub>3</sub> 60% 80% 60° respectively.

### 5.3. Load-concrete strain behaviour

Fig. 9 shows the load-strain behaviour for all beams' concrete in the compression zone. As can be observed, the control beam RCWS yields high concrete compressive strain as compared with the other beams at the same loads, while F<sub>4</sub> 45% 75% 40° yields lower concrete compressive strain until the load of 325 kN, beyond which the strain increases abruptly. The F<sub>2</sub> 60% 80%, 40°, and F<sub>3</sub> 60% 80% 60° curves show correspondence at the region from the load initiation till the load of 150 kN, after which the beam F<sub>2</sub> 60% 80% yields lower concrete compressive strain as compared with the other beams until failure. While the load-deflection behaviour shows that the beam F<sub>3</sub> 60% 80% 60° exhibited lower deflection than the F<sub>2</sub> 60% 80% at the same load during this stage. This can be explained by the variation in the movement of the neutral axis between the last two beams where the strain of the longitudinal steel reinforcement shows a nonuniform increase in the F<sub>3</sub> 60% 80% 60°. The RCWS strain profile is shown in Fig. 10. Finally, more or less similar behaviour has been observed in previous research work such as that of Kueres, Ricker and Hegger [23].

### 5.4. Shear ductility

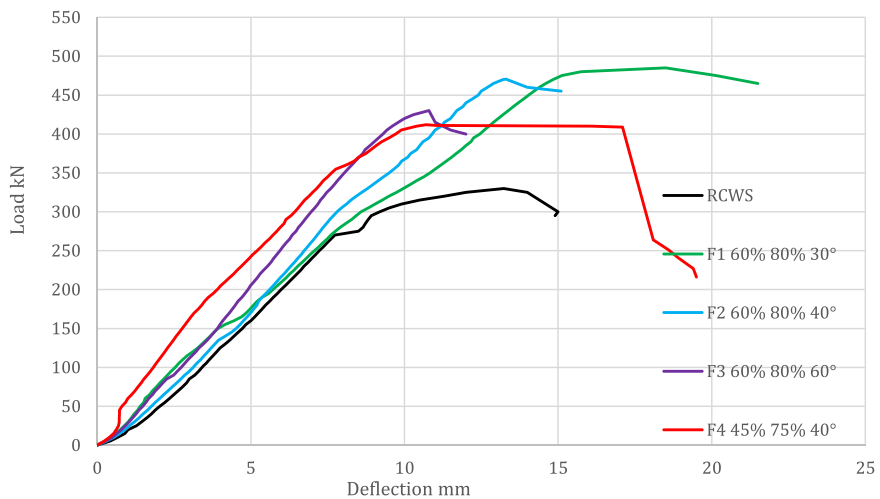
The representation of a broad understanding of ductility in structural engineering is the ability of the member to deform as the load continues to be applied after the maximum load stage [25]. Fig. 11 uses two different definitions of the shear ductility index ( $\mu$ ). The shear ductility index ( $\mu$ ) is computed by the ratio of the area under the load-deflection curve restraint up to 0.75 of the ultimate loads (0.75 Pmax) in the downward portion to the area up to the ultimate load (Pmax).

Table 6 shows the shear ductility index for all beams; "as can be observed, the shear ductility index increased gradually for F<sub>1</sub> 60% 80% 30°, F<sub>2</sub> 60% 80% 40°, and F<sub>4</sub> 45% 75% 40° by 4.13%, 5%, and 52% and decreased for F<sub>3</sub> 60% 80% 60° by about 8.26% as compared with the control beam RCWS. The beam F<sub>4</sub> 45% 75% 40° presented a clear enhancement in the shear ductility, indicating the flamingo technique's considerable influence" [24].

**Table 5**

Test results for the five beams.

Specimen	Ultimate load kN	$\Delta u$ mm	% Diff. in $\Delta u$
RCWS	330	13.2	–
F1 60% 80% 30°	485	18.5	40.15%
F2 60% 80% 40°	471	13.3	1%
F3 60% 80% 60°	430	10.8	-18.2%
F4 45% 75% 40°	412	10.7	-18.94%



**Fig. 8.** Load-deflection curves for all beams.

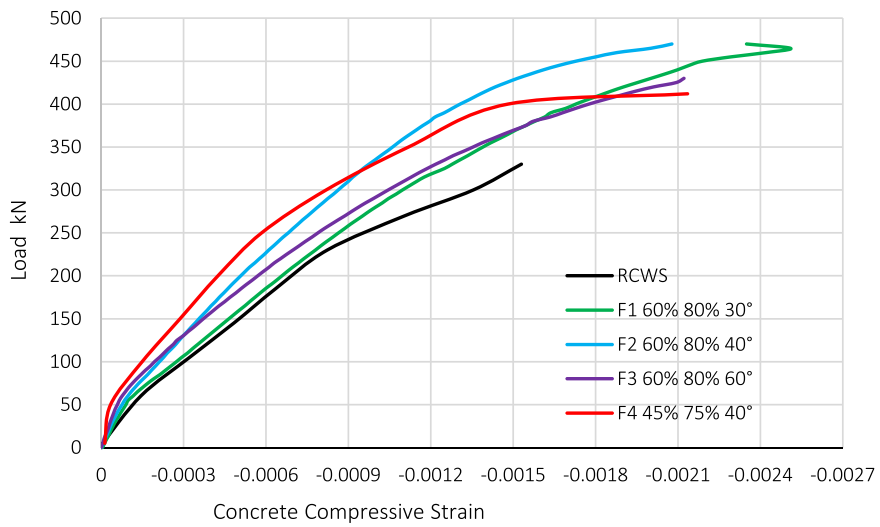


**Fig. 9.** Load-concrete compressive strain for all beams.

### 5.5. Cracking behaviour

The cracking details for all beams are presented in Table 7. “When the load has been applied on those beam specimens, the first crack has been formed at 16.66%, 12.3%, 14.5%, 16.2% and 14% from the ultimate load of RCWS, F<sub>1</sub> 60% 80% 30°, F<sub>2</sub> 60% 80% 40°, F<sub>3</sub> 60% 80% 60° and F<sub>4</sub> 45% 75% 40°, respectively. However, the cracking load is clearly increased with the use of the flamingo technique as compared with the traditional stirrups. The beams F<sub>2</sub> 60% 80% 40° and F<sub>3</sub> 60% 80% 60° showed higher cracking load as compared with the F<sub>1</sub> 60% 80% 30° and F<sub>4</sub> 45% 75% 40° for a reason for the higher ability to bend that both last two beams exhibited hence the concrete in the tensile zone cracked at lower load. The table also shows the crack width at the advanced loading stage. The crack width decreased for F<sub>1</sub> 60% 80% 30°, F<sub>2</sub> 60% 80% 40°, F<sub>3</sub> 60% 80% 60° and F<sub>4</sub> 45% 75% 40° by 4.8%, 46.3%, 26.8% and 14.63% as compared with the control beam. The cracks model behaves differently from one beam to another due to the change in the inclination angle of the free legs and the type of failure of the beam, the type of failure of the beam F<sub>1</sub> 60% 80% 30° was crushing in the concrete between the loading points, while F<sub>2</sub> 60% 80% 40° and F<sub>3</sub> 60% 80% 60° failed in shear-flexure and F<sub>4</sub> 45% 75% 40° in a pure flexure. Fig. 12 (a, b, c, d, and e) shows the failure modes of beams” [24].

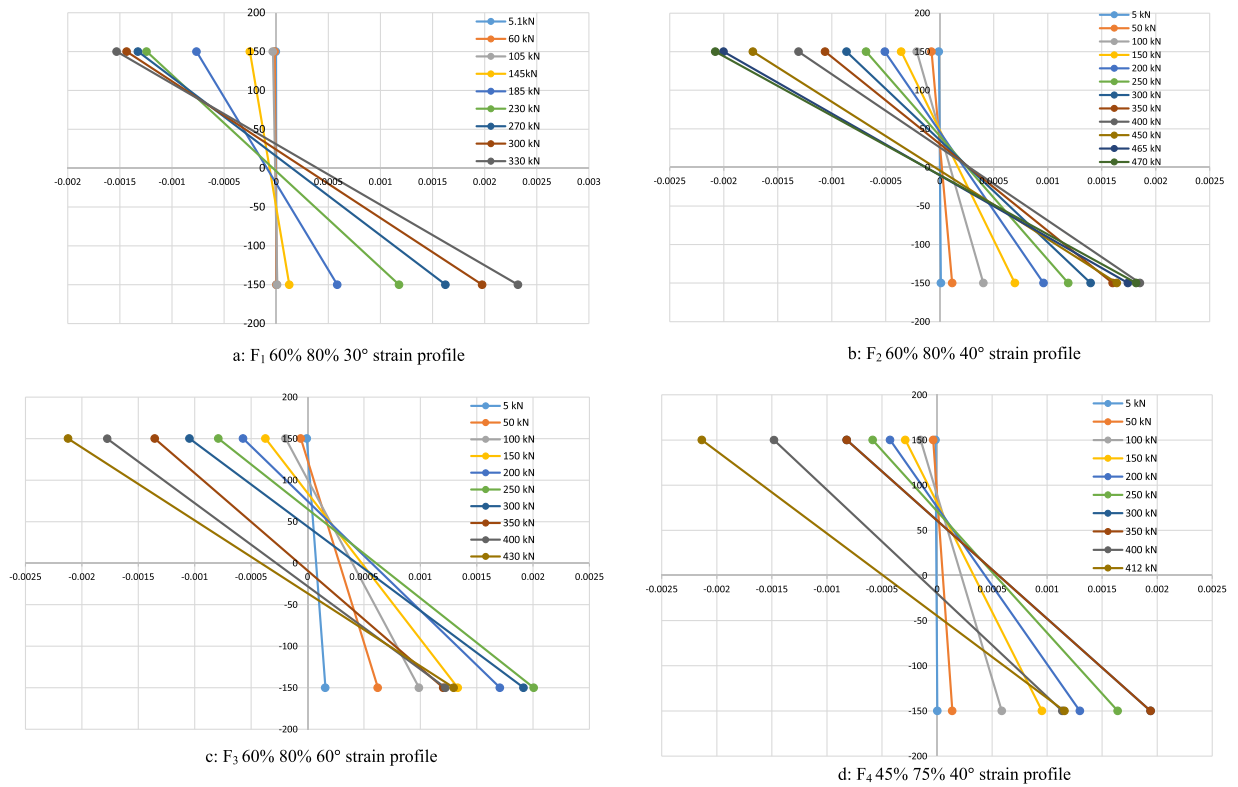


Fig. 10. Strain profile for all beams.

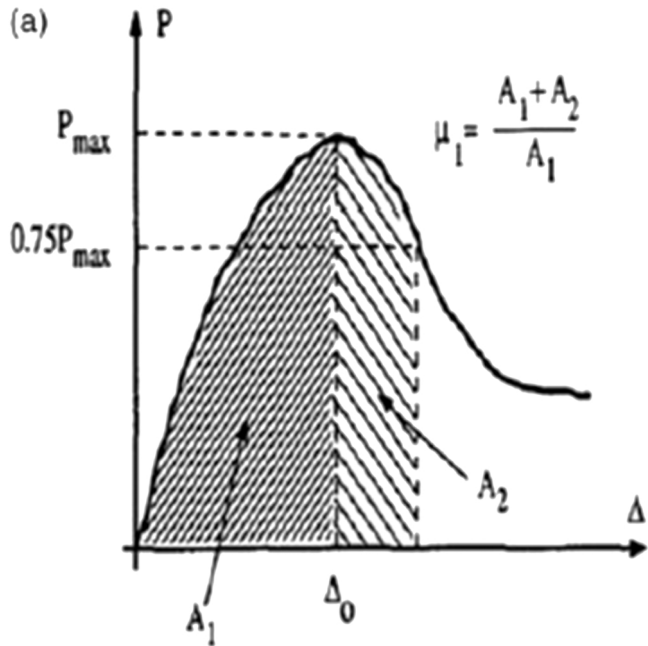


Fig. 11. The method of computing the shear ductility [26].

**Table 6**The index of the shear ductility ( $\mu_1$ ) of all beams.

Specimen	Ultimate load kN	$\Delta u$ mm	Index of Shear ductility ( $\mu_1$ )	Increase in the shear ductility (%)
RCWS	330	13.2	1.21	–
RCWOS	266	7.29	1.22	–
F1 60% 80% 30°	485	18.5	1.26	4.13%
F2 60% 80% 40°	471	13.3	1.27	5%
F3 60% 80% 60°	430	10.8	1.11	-8.26%
F4 45% 75% 40°	412	10.7	1.84	52%

**Table 7**

The cracks details for all specimens.

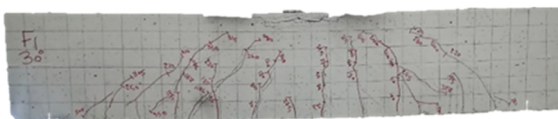
Specimen	Crack load Pcr (kN)	Ultimate load Pu (kN)	Pcr/Pu (%)	Ultimate crack width Wu (mm)
RCWS	55	330	16.66%	0.065
F1 60% 80% 30°	60	485	12.3%	0.06
F2 60% 80% 40°	68	471	14.5%	0.11
F3 60% 80% 60°	70	430	16.2%	0.15
F4 45% 75% 40°	58	412	14%	0.115

## 6. Conclusions

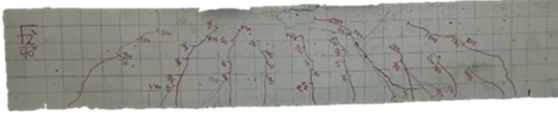
1. The flamingo technique showed better results than the traditional steel stirrups in terms of load-deflection behaviour, post-cracking stiffness, cracking behaviour, and crack width.
2. The flamingo technique with 30° inclination yields high load-carrying capacity and larger deflection; hence it is considered the optimum case of this technique.
3. The F4 45% 75% 40° showed lower load-carrying capacity, lower ultimate deflection, higher post-cracking strength, and a higher shear ductility index.
4. The variation in the movement of the neutral axis for both F2 60% 80% 40° and F3 60% 80% 60°. This explained the conflict between load-deflection and load-strain behaviour.



a: Crack pattern for RCWS



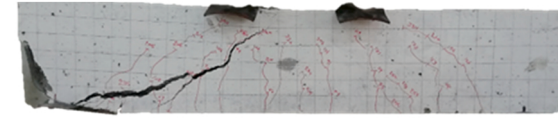
b: Crack pattern for F1 60% 80% 30°



c: Crack pattern for F2 60% 80% 40°



d: Crack pattern for F3 60% 80% 60° strain profile



e: Crack pattern for F4 45% 75% 40°

**Fig. 12.** Crack pattern for all beams.

5. The reduction in the length of the lower free end by 15% leads to a decrease in the load-carrying capacity.
6. Both F<sub>3</sub> 60% 80% 60° and F<sub>4</sub> 45% 75% 40° showed shear failure, while F<sub>2</sub> 60% 80% 40° failed in a shear-flexure and F<sub>1</sub> 60% 80% 30° in pure flexure.

## CRediT authorship contribution statement

**Suhad M. Abd:** Conception and design of study, Drafting the manuscript, Approval of the version of the manuscript to be published. **Isam S. Mhaimeed:** Conception and design of study, Drafting the manuscript, Approval of the version of the manuscript to be published. **Bassam A. Tayeh:** analysis and/or interpretation of data, revising the manuscript critically for important intellectual content, Approval of the version of the manuscript to be published. **Hadee Mohammed Najim:** acquisition of data, revising the manuscript critically for important intellectual content, Approval of the version of the manuscript to be published. **Shaker Qaidi:** Conception and design of study, Drafting the manuscript, Approval of the version of the manuscript to be published.

## Declaration of Competing Interest

The authors declare that they have no known competing financial interests or personal relationships that could have appeared to influence the work reported in this paper.

## Data availability

No data was used for the research described in the article.

## Acknowledgements

The authors would like to thank the staff of the structure lab of the civil dept. In the College of Engineering at Diyala Univ.-IRAQ for the help, they have provided.

## References

- [1] A.M. Ibrahim, Z.S. Khaled, I.M.A. Ameer, Effect of using internal steel plates for shear reinforcement on flexural behavior of self-compacting concrete beams, *Al-Nahrain J. Eng. Sci.* 20 (5) (2017) 1071–1082.
- [2] M.H. Akeed, S. Qaidi, H.U. Ahmed, W. Emad, R.H. Faraj, A.S. Mohammed, B.A. Tayeh, A.R.G. Azevedo, Ultra-high-performance fiber-reinforced concrete. Part III: fresh and hardened properties, *Case Stud. Constr. Mater.* 17 (2022), e01265.
- [3] B.A. Tayeh, M.H. Akeed, S. Qaidi, B.H.A. Bakar, Influence of sand grain size distribution and supplementary cementitious materials on the compressive strength of ultrahigh-performance concrete, *Case Stud. Constr. Mater.* 17 (2022), e01495.
- [4] S.N. Ahmed, N. Hamah Sor, M.A. Ahmed, S.M.A. Qaidi, Thermal conductivity and hardened behavior of eco-friendly concrete incorporating waste polypropylene as fine aggregate, *Mater. Today Proc.* 57 (2022) 818–823.
- [5] Y.I.A. Aisheh, D.S. Atrush, M.H. Akeed, S. Qaidi, B.A. Tayeh, Influence of steel fibers and microsilica on the mechanical properties of ultra-high-performance geopolymers concrete (UHP-GPC), *Case Stud. Constr. Mater.* 17 (2022), e01245.
- [6] M.H. Akeed, S. Qaidi, H.U. Ahmed, R.H. Faraj, S.S. Majeed, A.S. Mohammed, W. Emad, B.A. Tayeh, A.R.G. Azevedo, Ultra-high-performance fiber-reinforced concrete. Part V: mixture design, preparation, mixing, casting, and curing, *Case Stud. Constr. Mater.* 17 (2022), e01363.
- [7] M.H. Akeed, S. Qaidi, H.U. Ahmed, R.H. Faraj, A.S. Mohammed, W. Emad, B.A. Tayeh, A.R.G. Azevedo, Ultra-high-performance fiber-reinforced concrete. Part II: hydration and microstructure, *Case Stud. Constr. Mater.* 17 (2022), e01289.
- [8] A. Borri, M. Corradi, G. Castori, A. Molinari, Stainless steel strip—a proposed shear reinforcement for masonry wall panels, *Constr. Build. Mater.* 211 (2019) 594–604.
- [9] R.Z. Al-Rousan, Integration of CFRP strips as an internal shear reinforcement in reinforced concrete beams exposed to elevated temperature, *Case Stud. Constr. Mater.* 14 (2021), e00508.
- [10] M.U. Khan, M. Fahad, K. Shahzada, Shear capacity assessment of reinforced concrete beams using swimmer bars as shear reinforcement, *SSRG Int. J. Civ. Eng.* 2 (6) (2015) 14–20.
- [11] M.H. Akeed, S. Qaidi, H.U. Ahmed, R.H. Faraj, A.S. Mohammed, W. Emad, B.A. Tayeh, A.R.G. Azevedo, Ultra-high-performance fiber-reinforced concrete. Part IV: Durability properties, cost assessment, applications, and challenges, *Case Stud. Constr. Mater.* 17 (2022), e01271.
- [12] M.M. Al-Tayeb, Y.I.A. Aisheh, S.M.A. Qaidi, B.A. Tayeh, Experimental and simulation study on the impact resistance of concrete to replace high amounts of fine aggregate with plastic waste, *Case Stud. Constr. Mater.* 17 (2022), e01324.
- [13] T.S. Al-Gasham, J.M. Mhalhal, S.R. Abid, Flexural behavior of laced reinforced concrete moderately deep beams, *Case Stud. Constr. Mater.* 13 (2020), e00363.
- [14] M. Al-Nasra, I. Duweib, A. Najmi, The use of pyramid swimmer bars as punching shear reinforcement in reinforced concrete flat slabs, *J. Civ. Eng. Res.* 3 (2) (2013) 75–80.
- [15] P. Srinivasa Rao, B. Sarma, N. Lakshmanan, F. Stangenberg, Seismic behavior of laced reinforced concrete beams, in: Proceedings of the Eleventh World Conference on Earthquake Engineering, 1996.
- [16] J. Ahmad, K.J. Kontoleon, A. Majdi, M.T. Naqash, A.F. Deifalla, N. Ben Kahla, H.F. Isleem, S.M.A. Qaidi, A comprehensive review on the ground granulated blast furnace slag (GGBS) in concrete production, *Sustainability* 14 (14) (2022) 8783.
- [17] S.M.A. Qaidi, B.A. Tayeh, A.M. Zeyad, A.R.G. de Azevedo, H.U. Ahmed, W. Emad, Recycling of mine tailings for the geopolymers production: a systematic review, *Case Stud. Constr. Mater.* 16 (2022), e00933.
- [18] A. Saeed, H.M. Najim, A. Hassan, S. Qaidi, M.M.S. Sabri, N.S. Mashaan, A. Comprehensive, Study on the effect of regular and staggered openings on the seismic performance of shear walls, *Buildings* 12 (9) (2022) 1293.
- [19] C. Madheswaran, G. Gnanasundar, N. Gopalakrishnan, Performance of laced reinforced geopolymer concrete (LRGPC) beams under monotonic loading, *Adv. Struct. Eng.* (2015) 355–367.
- [20] I. Almeshal, M.M. Al-Tayeb, S.M.A. Qaidi, B.H. Abu Bakar, B.A. Tayeh, Mechanical properties of eco-friendly cements-based glass powder in aggressive medium, *Mater. Today Proc.* 58 (2022) 1582–1587.
- [21] S.M.A. Qaidi, Y.Z. Dinkha, J.H. Haido, M.H. Ali, B.A. Tayeh, Engineering properties of sustainable green concrete incorporating eco-friendly aggregate of crumb rubber: a review, *J. Clean. Prod.* 324 (2021), 129251.
- [22] A.A. Allawi, N.S. Arshad, Behavior of laced reinforced concrete beam under static load, *J. Eng. Sustain. Dev.* 21 (03) (2017), 2520-0917.

- [23] D. Kueres, I.M. Ricker, J. Hegger, A new punching shear reinforcement system for precast footings, in: Proceedings of the 2016 PCI Convention & National Bridge Conference, Nashville, USA, 2016.
- [24] I.S. Mhaimeed, S.M. Abd, Shear capacity of concrete beams reinforced with textile carbon yarns and flamingo reinforcing system, in: Proceedings of the 4th International Iraqi Conference on Engineering Technology and Their Applications (IICETA), 2021, pp. 212–217.
- [25] R. Narayan, I. Darwish, Fiber concrete deep beams in shear, Struct. J. 85 (2) (1988) 141–149.
- [26] Y. Xie, S.H. Ahmad, T. Yu, S. Hino, W. Chung, Shear ductility of reinforced concrete beams of normal and high-strength concrete, Struct. J. 91 (2) (1994) 140–149.